



Published in final edited form as:

J Clin Cell Immunol. ; 5: 259–. doi:10.4172/2155-9899.1000259.

Tyrosine Kinase Inhibition Regulates Early Systemic Immune Changes and Modulates the Neuroimmune Response in α -Synucleinopathy

Michaeline L. Hebron¹, Irina Lonskaya¹, Paul Olopade¹, Sandra T. Selby², Fernando Pagan^{3,4}, and Charbel E-H Moussa^{1,3,*}

¹Department of Neuroscience, Laboratory for Dementia and Parkinsonism, Georgetown University Medical Center, Washington D.C., 20007, USA

²Department of Oncology, Lombardi Cancer Center, Georgetown University Medical Center, Washington D.C., 20007, USA

³Neurorestoration Group, Movement Disorders Program, National Parkinson Foundation Center of Excellence, Georgetown University Hospital, Washington D.C., 20007, USA

⁴Department of Neurology, Georgetown University Hospital, Washington D.C., 20007, USA

Abstract

Objectives—Neuro-inflammation is common in α -Synucleinopathies and Tauopathies; and evidence suggests a link between the tyrosine kinase Abl and neurodegeneration. Abl upregulates α -Synuclein and promotes Tau hyper-phosphorylation (p-Tau), while Abl inhibitors facilitate autophagic clearance.

Methods—A model of α -Synucleinopathy harboring human mutant A53T α -Synuclein and exhibits concomitant increase in murine p-Tau was used to determine the immunological response to Abl inhibition.

Results—Age-dependent alterations of brain immunity, including loss of IL-10 and decreased levels of IL-2 and IL-3 were observed in old A53T mice. Brain CCL2 and CCL5 were decreased, but CX3CL1 remained constantly elevated. Young A53T mice exhibited differential systemic and central immune profiles in parallel with increased blood markers of adaptive immunity, suggesting an early systemic immune response. Tyrosine kinase inhibitors (TKIs), including nilotinib and

Copyright: © 2014 Hebron ML, et al.

This is an open-access article distributed under the terms of the Creative Commons Attribution License, which permits unrestricted use, distribution, and reproduction in any medium, provided the original author and source are credited.

*Corresponding author: Charbel E-H. Moussa, MB. Ph.D., Department of Neuroscience, Georgetown University School of Medicine, 3970 Reservoir Rd, NW, TRB, Room WP09B, Washington DC 20057, USA, Tel: 202-687-7328; Fax: 202-687-0617; cem46@georgetown.edu.

Authors Contributions

Michaeline L. Hebron, injected the mice and performed ELISA and Milliplex, Irina Lonskaya performed immunohistochemistry, Paul Olopade provided literature search and organized data, Sandra T. Selby, performed Milliplex and Fernando Pagan edited the manuscript. Charbel E-H Moussa designed the experiments and wrote the manuscript.

Conflict of Interest

Dr. Charbel Moussa has a provisional patent application to use nilotinib and bosutinib to treat neurodegenerative diseases. Other authors declare no conflict of interest in association with this manuscript.

bosutinib reduced brain and peripheral α -Synuclein and p-Tau and modulated blood immunological responses. TKIs did not affect brain IL-10, but they changed the levels of all measured blood immune markers, except CX3CL1. TKIs altered microglia morphology and reduced the number of astrocyte and dendritic cells, suggesting beneficial regulation of microglia.

Conclusions—These data indicate that tyrosine kinase inhibition affects neuro-inflammation via early changes of the peripheral immune profile, leading to modulation of the neuro-immune response to α -Synuclein and p-Tau.

Keywords

Microglia; Tau; α -Synuclein; Nilotinib; Bosutinib; Inflammation; Abl

Background

Inflammation is reported in several neurodegenerative diseases, including Parkinson (PD), Alzheimer (AD) and the Tauopathies [1]. The inflammatory response is thought to generally localize to areas of central nervous system (CNS) injury via communication between immune cells and stressed neurons. It was initially thought that α -Synuclein-related pathology was confined to within neurons, but recent work suggests that microglia are activated following the release of α -Synuclein into the extracellular space [2]. Aggregated forms of α -Synuclein induce microglia activation [3,4], suggesting that this may be one of the mechanisms of neurodegeneration [5,6]. Activated microglia are present in postmortem brains of patients with primary Tauopathies, including fronto-temporal dementia with parkinsonism linked to chromosome-17 (FTDP), progressive supranuclear palsy (PSP) and corticobasal degeneration (CBD) [7–9]. We demonstrated microglia activity and p-Tau accumulation in α -Synuclein gene transfer models [10] and conversely, α -Synuclein phosphorylation and accumulation together with p-Tau in lentiviral Tau models [10,11]. Cell culture models also demonstrate that pro-inflammatory cytokines can induce p-Tau [12–14]; and the endotoxin lipopolysaccharide (LPS) promotes inflammation and p-Tau accumulation [15], while suppression of microglia activity prolongs survival in Tau mutant P301L transgenic mice [16]. These findings suggest that microglia activity is associated with p-Tau and α -Synuclein through an underlying mechanism moderating communication between microglia and neurons.

The non-receptor tyrosine kinase Abelson (Abl) has been linked to inflammation in neurodegenerative diseases and animal models of neurodegeneration [17–19]. We demonstrated that Abl activation increases α -Synuclein levels in mutant A53T mice and α -Synuclein gene transfer models [20,21]. Recent findings in rat models showed that Abl activation is also associated with α -Synuclein phosphorylation [22], which may be linked to protein aggregation [10]. In AD, Abl is also associated with neurofibrillary tangles (NFTs) [23–26], and it is activated in the hippocampus and entorhinal cortex in post-mortem brains [23,24]. Src tyrosine kinase is also recognized in AD via interaction with Tau [27–29]. We demonstrated that tyrosine kinase inhibitors (TKIs), including nilotinib and bosutinib penetrate the brain and inhibit Abl, resulting in a decrease of α -Synuclein [20–22,30] and p-Tau levels [20,21,30–33]. Nilotinib (AMN107) is a second generation selective Bcr-Abl inhibitor, which is clinically effective in adult chronic myeloid leukemia (CML) [34].

Because Src and Abl are structurally homologous, the dual Src/Abl TKI bosutinib (SKI-606) can also inhibit Abl [35].

Microglia activation has been extensively studied in the pathogenesis of neurodegenerative disorders; and the role of adaptive and innate CNS immunity is a growing area of interest. However, determining the temporal interaction between systemic and CNS immunity in response to protein accumulation is critical to understanding the beneficial or detrimental role of microglia activity at different stages of disease. These studies investigated the temporal changes of peripheral and CNS innate and adaptive immune response in mutant A53T α -Synuclein mice that exhibit murine p-Tau accumulation [21,36] with and without TKI-induced reduction of α -Synuclein and p-Tau. We followed the same treatment paradigm that we previously published using 10 mg/kg nilotinib or 5 mg/kg bosutinib every other day for 6 weeks [20–22,30]. We found that peripheral systemic inflammatory markers, reflecting the interplay between innate and adaptive immunity, change in parallel with CNS immunity; and these changes are reversed by nilotinib and bosutinib. The current studies suggest communication between peripheral and CNS immunity to modulate the inflammatory brain response to α -Synuclein and p-Tau.

Methods

Nilotinib and bosutinib treatment

Transgenic mice harboring the A53T mutation of α -Synuclein [36] and age-matched C57BL/6 mice (WT) were treated with intraperitoneal (I.P) injection of either 10 mg/kg nilotinib or 5 mg/kg bosutinib or 3 μ L dimethylsulfoxide (DMSO) every other day for 6 weeks. All animal experiments were conducted in full compliance with the recommendations of Georgetown University Animal Care and Use Committee (GUAUC). n=20 animals were used for immunohistochemistry, n=15 for longitudinal studies, n=12 were used for brain and blood extraction, n=20 were used for organ extraction and n=40 were used for drug treatment. All graphs and statistical analyses were performed in Graph Pad Prism Software (Graph Pad Prism Software, Inc. CA. USA). All statistics were performed using ANOVA with Newman–Keuls multiple comparison test and data were expressed as Mean \pm SD.

Tissue collection and Milliplex enzyme-linked immunosorbent assay (ELISA)

Animals were deeply anesthetized with a mixture of Xylazine and Ketamine (1:8), and 50–150 μ L of whole blood was collected via cardiac puncture, centrifuged at 15000 \times g to precipitate blood cells and the supernatant was examined by ELISA. To wash out the remaining blood from vessels and reduce contamination, animals were perfused with 10 ml of 1X saline for 4 min and the brain, spleen, heart, gastrocnemius muscle and small intestine were collected and immediately homogenized in 0.5 ml ELISA buffer. We customized a highly sensitive and unbiased Milliplex[®] MAP Kit (Cat # MPXMCYTO-70K, Millipore) with color-coded microspheres (beads) and fluorescent dyes, which through precise concentrations, the beads can simultaneously and specifically capture mouse cytokines, including IL6, IL-1 α , IL-1 β , TNF- α , IL-2, IL-3, IL-4, IL-10, VEGF, IFN- γ , CCL2, and CCL5. A total of 25 μ L of sample was introduced into a plate containing the microspheres

and the reaction mixture was incubated with Streptavidin-PE conjugate and the reporter molecule as described in the manufacturer's protocol. Using a Luminex[®] machine, microspheres are first passed through a laser which excites the internal dyes making the microspheres; and a second laser that excites the PE, which is the fluorescent dye on the reporter molecule, and then a high speed digital-signal processor identifies each individual microsphere and quantifies the bioassay.

Immunohistochemistry of brain sections

Animals were deeply anesthetized with a mixture of Xylazine and Ketamine (1:8), washed with 1X saline for 1 min and then perfused with 4% paraformaldehyde (PFA) for 15–20 min. Brains were quickly dissected out and immediately stored in 4% PFA for 24 h at 4°C, and then transferred to 30% sucrose at 4°C for 48 h. Brains were cut using a cryostat at 4°C into 20-micron-thick coronal sections and stored at -20°C. Immunohistochemistry was performed on 20 µm-thick sections. Astrocytes were probed (1:200) with monoclonal anti-GFAP antibody (Millipore Corporation, USA), and microglia were probed (1:200) with IBA-1 polyclonal antibody (Wako, USA). Dendritic cells and/or microglia were probed (1:200) with CD11b polyclonal antibodies (Thermo Fisher, USA). Nuclear staining with 4', 6-Diamidino-2-Phenylindole (DAPI) was performed according to manufacturer's protocols (Life Technologies, USA).

Stereological methods

Stereological methods were applied by a blinded investigator using unbiased stereology analysis (Stereologer, Systems Planning and Analysis, Chester, MD) to determine the total positive cell counts in 20 striatal fields on at least 10 brain sections (~400 positive cells per animal) from each animal. These areas were selected across different regions on either side from the point of injection and all values were averaged to account for the gradient of staining across 1 mm radius from the point of injection. An optical fractionator sampling method was used to estimate the total number of positive cells with multi-level sampling design. Cells were counted within the sampling frame determined optically by the fractionator and cells that fell within the counting frame were counted as the nuclei came into view while focusing through the z-axis.

Caspase-3 fluorometric activity assay

To measure caspase-3 activity in the animal models, we used EnzChek[®] caspase-3 assay kit #1 (Invitrogen) on cortical extracts and Z-DEVD-AMC substrate and the absorbance was read according to manufacturer's protocol.

CX3CL1 ELISA

Mouse CX3CL1 (Cayman) ELISA was performed using 50 µl (1 µg/µl) total brain or blood lysates, which was detected with CX3CL1 primary antibody (3 h) and 100 µl anti-rabbit antibody (30 min) at RT. Extracts were incubated with stabilized Chromogen for 30 min at RT and solution was stopped and read according to manufacturer's protocol.

Human α -Synuclein and p-Tau ELISA

Human α -Synuclein and p-Tau ELISA were performed using 50 μ l (1 μ g/ μ l) of brain lysates detected with 50 μ l primary antibody (3 h) and 100 μ l anti-rabbit secondary antibody (30 min) at RT. α -Synuclein levels were measured using human specific ELISA (Invitrogen) according to manufacturers' protocols. p-Tau was measured using specific p-Tau at serine 396 according to manufacturer's protocol.

Results

Age-dependent alterations of brain immunity in A53T mice

Age-dependent studies (Figure 1A) showed that A53T mice accumulate a significant level of α -Synuclein (n=5, p<0.01) and serine 396 p-Tau (n=5, p<0.05) as early as 2–3 months of age (Figure 1) compared to wild type (WT) C57BL/6 mice; and these levels increase further at 10 months (n=5, p<0.001), suggesting α -Synuclein and p-Tau accumulation in total brain extracts. It is important to mention that no α -Synuclein or p-Tau is expressed in the substantia nigra in A53T mice [21,36]. Caspase-3 activation was also significantly increased in young (2–3 months) and older (10 months old) A53T mice (Figure 1B, n=5, p<0.05).

Age-dependent loss of modulators of the immunological memory

We used a highly sensitive unbiased milliplex ELISA to simultaneously measure changes in inflammatory markers in the whole blood and total brain lysates of A53T mice. Significant increases in brain pro-inflammatory cytokines, including interleukin (IL)-6 and IL-1 β (n=5, p<0.05), and a decrease in IL-1 α (p<0.01) were detected in 2–3 months A53T old mice compared to WT (Figure 1C). No differences were observed in inflammatory profiles between young and older WT mice in these experiments, so WT mice were presented as one age group. No changes in tumor necrosis factor- α (TNF- α) were observed in young A53T (2–3 months) mice, but TNF- α significantly dropped at 10 months (p<0.01). Pro-inflammatory cytokines, including IL-1 α and 1 β returned to WT level (Figure 1C) and IL-6 significantly decreased below WT levels (n=5, p<0.001). IL-10 in A53T mice was significantly increased (Figure 1D, n=5, p<0.01) at 2–3 months, while both IL-4 and IL-10 were significantly decreased at 10 months (p<0.001), suggesting loss of immunosuppression after prolonged periods of α -Synuclein and p-Tau accumulation. IL-2, which is implicated in T-cell (CD4⁺ and CD8⁺) proliferation, was also significantly decreased at 2–3 months (Figure 1E, n=5, p<0.001) and both IL-2 (p<0.001) and IL-3 (p<0.0001), which may stimulate proliferation of myeloid lineage cells [37], were significantly decreased at 10 months in A53T mice (Figure 1E) compared to WT. Furthermore, interferon (IFN)- γ which is also critical for innate and adaptive immunity [38,39], was significantly decreased at 10 months (Figure 1F, n=5, p<0.01), while Vascular Endothelial Growth Factor (VEGF), which is secreted by endothelial cells and stimulates vasculogenesis and angiogenesis in response to brain injury [40–44] was significantly increased (p<0.001) at 2–3 months in A53T mice and returned to WT level at 10 months (Figure 1F).

Chemokine (C-C motif) ligand 2 (CCL2) or the monocyte chemotactic protein-1 (MCP-1) recruits monocytes, memory T cells, and dendritic cells to the sites of injury [45,46]. CCL5 is another chemotactic for T cells, eosinophils, and basophils, and plays an active role in

recruiting leukocytes into inflammatory sites [47,48]. CCL5 was significantly decreased in the brain of 2–3 months old A53T mice (Figure 1G, n=5, p<0.01), and further decrease was observed at 10 months in both CCL2 (n=5, p<0.05) and CCL5 (p<0.001) compared to WT. Soluble fractalkine (CX3CL1) attracts T cells and monocytes, while the cell-bound chemokine promotes adhesion of leukocytes to activated endothelial cells [49]. Importantly, several reports indicated a relationship between CX3CL1, which is expressed on neurons, and microglia activity in neurodegeneration [50,51], particularly in relation to Tau pathology [52,53]. Interestingly, CX3CL1 was significantly increased in the brain of 2–3 months old A53T mice (Figure 1G, n=5, p<0.05) and remained high at 10 months of age compared to WT.

Differential profiles of systemic and central immunity in A53T mice

Because we observed increased levels of inflammatory cytokines in 2–3 months old A53T mice inflammatory markers were measured in as early as 1–2 month old mice in total blood and brain lysates. Only IL-1 α was significantly increased in A53T brains (Figure 2A, n=4, p<0.05) compared to WT, while IL-1 α was decreased (p<0.05) and IL-1 β was increased in A53T blood (Figure 2A, p<0.05) compared to WT. IL-10 was also significantly increased in the brain (Figure 1B, n=4, p<0.001) and the blood (p<0.05), but IL-4 did not change. A53T brain levels of VEGF were significantly increased compared to WT (Figure 2C, n=4, p<0.01) and IFN- γ was decreased (p<0.05) compared to WT. VEGF levels in total blood of A53T mice were increased (p<0.05) compared to WT. These data suggest changes in the blood immune profile simultaneously with alterations of CNS immune markers. However, while IL-3 was decreased in the A53T brain (Figure 2D, n=4, p<0.05) compared to WT, IL-2 was significantly increased in the blood (p<0.05) compared to WT, suggesting enhanced adaptive immunity in the blood. Additionally, CCL2 was significantly decreased in A53T brains (Figure 2E, n=4, p<0.05) compared to WT, but significant increases in CCL5 (p<0.05) and CX3CL1 (p<0.01) were observed in the A53T blood compared to WT, suggesting altered systemic chemotactic activities.

Nilotinib and bosutinib decrease CNS and peripheral levels of α -Synuclein and p-Tau. Transgenic A53T mice were intraperitoneally (I.P) injected with either 10 mg/kg nilotinib or 5 mg/kg bosutinib or 3 μ L dimethylsulfoxide (DMSO) every other day for 6 weeks as we previously described [20–22,30]. We previously demonstrated that nilotinib and bosutinib penetrate the brain, inhibit Abl activity and induce autophagic clearance of α -Synuclein and p-Tau in A53T mice and lentiviral gene transfer models [20,21,30,32,33].

Here we show the effects of TKIs on α -Synuclein and p-Tau in brain and peripheral tissue in 2–3 months old A53T and WT mice treated with TKIs every other day for 6 weeks. No differences in immunological profiles were observed in WT mice between DMSO, nilotinib and bosutinib treatment, so WT data were presented as only WT. As we previously demonstrated, α -Synuclein was significantly increased (Figure 2F, n=4, p<0.01) in A53T brains compared to WT, and this increase was greater (n=4, p<0.001) in older mice. However, both nilotinib and bosutinib reduced α -Synuclein levels (p<0.01) in young as well as older (p<0.01) A53T mice, which remained higher than WT. p-Tau (ser 396) was also significantly increased (Figure 2F, n=4, p<0.05) in young A53T brains compared to WT,

and this increase was greater ($n=4$, $p<0.0001$) in older mice. Nilotinib and bosutinib reversed p-Tau levels ($p<0.05$) in young as well as older ($p<0.001$) A53T mice, which remained higher than WT. Nilotinib and bosutinib also prevented the increase of caspase-3 activity that was detected in young and old A53T mice treated with DMSO (Figure 2G, $p<0.05$) compared to WT mice. Both nilotinib and bosutinib significantly reduced p-Tau levels, which remained higher than control. α -Synuclein was also significantly increased in 3–4 month old A53T mice peripheral tissues, including muscle (gastrocnemius), small intestine and blood (Figure 3A, $n=4$, $p<0.05$) compared to WT, and nilotinib and bosutinib reversed α -Synuclein levels. Similarly, p-Tau levels were also significantly increased in muscle, small intestine and blood (Figure 3B, $n=4$, $p<0.05$) of 3–4 months old A53T mice compared to WT, and nilotinib and bosutinib reduced p-Tau. No effects of TKIs were observed on total α -Synuclein or p-Tau levels in WT mice. The decrease in α -Synuclein and p-Tau (threonine 231) levels were further verified by WB analysis that show a significant increase in α -Synuclein and p-Tau in the small intestine and gastrocnemius muscle of A53T mice with DMSO compared to WT (Figure 3C, $p<0.05$, $n=4$). However, nilotinib and bosutinib reduced the levels of both α -Synuclein and p-Tau back to WT levels, suggesting TKI effects on peripheral tissue.

Nilotinib and bosutinib modulate changes in blood immunological profiles of A53T mice. To determine the effects of α -Synuclein and p-Tau clearance in 1–2 months old mice, immune markers were measured in whole blood and total brain lysates after 6 week trials with TKIs. Only IL-1 α was significantly reduced in the A53T brain (Figure 3D, $n=4$, $p<0.05$) compared to WT, and nilotinib and bosutinib reversed this effect in A53T but had no effects on WT mice (data not shown). However, the levels of IL-1 α and IL-1 β was significantly increased in the A53T blood (Figure 3F, $n=5$, $p<0.05$) compared to WT, and nilotinib and bosutinib reversed IL-1 α and 1 β levels back to WT, and significantly decreased IL-6 ($p<0.05$) compared to WT. Moreover, IL-10 was significantly increased in the A53T brain (Figure 3F, $n=4$, $p<0.05$) compared to WT, but neither nilotinib nor bosutinib altered the level of brain IL-10 in A53T brains, but they reversed it back to WT in the blood (Figure 3G, $n=4$, $p<0.05$), suggesting that TKIs may be able to differentially modulate pro-and anti-inflammatory innate immune changes in the blood and the brain. Furthermore, bosutinib significantly reduced IL-2 in the A53T brain (Figure 4A, $n=5$, $p<0.05$) compared to DMSO and WT. IL-2 was significantly increased in A53T blood ($p<0.05$) compared to WT, and both nilotinib and bosutinib reversed the increase of IL-2 in the blood of A53T mice back to WT level (Figure 4B, $n=4$, $p<0.05$). Nilotinib and bosutinib did not change the decrease of IL-3 levels in A53T brains (Figure 4A) but nilotinib reversed IL-3 increase in A53T blood (Figure 4B, $n=4$, $p<0.05$) and bosutinib reduced it below WT levels ($p<0.05$). Nilotinib and bosutinib did not affect the alteration of VEGF and IFN- γ in A53T brains compared to WT (Figure 4C, $n=4$, $p<0.05$), but they reversed the significant increase of VEGF in A53T blood compared to WT (Figure 4D, $n=4$, $p<0.05$). No significant changes were observed in CCL2 and CCL5 in A53T compared to WT brains (Figure 4E, $n=4$), but CX3CL1 was increased in A53T brains compared to WT (Figure 4E, $n=4$, $p<0.05$) and nilotinib and bosutinib reversed this increase back to WT level. However, CCL5 was significantly increased in A53T blood compared to WT (Figure 4F, $n=4$, $p<0.05$) and nilotinib and bosutinib abrogated this effect.

Blood CX3CL1 was significantly increased in A53T blood compared to WT mice (Figure 4F, n=4, p<0.001) and nilotinib and bosutinib failed to change CX3CL1 levels in the blood.

Nilotinib and bosutinib alter microglia morphology and reduce astrocyte and dendritic cells count. Immuno-histological staining showed increased number of ionized calcium-binding adapter (IBA)-1 positive microglia in the striatum of 3–4 months old A53T mice (Figure 5B, n=4) compared to WT (Figure 5A, n=4). Stereological counting showed a significant increase in microglial number in A53T striatum compared to WT (Figure 5E, n=4, p<0.05), and either bosutinib (Figure 5C, n=4) or nilotinib (Figure 5D, n=4) significantly increased the number of IBA-1-positive microglia (Figure 5E, p<0.01) compared to DMSO. Interestingly, microglia predominantly displayed an amoeboid-like morphology in DMSO treated A53T striatum (Figure 5B, insert) but this morphology appeared ramified after bosutinib (Figure 5C, insert) and nilotinib (Figure 5D, insert) treatment. Glial Fibrillary Acid Protein (GFAP) staining showed increased number of reactive astrocytes in the striatum of 3–4 months old A53T mice (Figure 5G, n=4) compared to WT (Figure 5F, n=4). Stereological counting showed a significant increase in reactive astrocytes in A53T striatum compared to WT (Figure 5J, n=4, p<0.01), and either bosutinib (Figure 5H, n=4) or nilotinib (Figure 5I, n=4) reversed GFAP staining back to WT levels. CD11b staining showed increased number of dendritic cells in the A53T striatum (Figure 5L, n=4) compared to WT (Figure 5K, n=4) and stereological counting showed a significant increase in CD11b-positive cells in A53T compared to WT (Figure 5O, n=4, p<0.001), and bosutinib (Figure 5M, n=4) or nilotinib (Figure 5N, n=4) reversed CD11b staining, which remained higher than WT levels (p<0.05).

Discussion

These studies provide insights into the systemic immune response and its potential role in modulating innate and adaptive immunity in the brain in α -Synucleinopathies. α -Synuclein and p-Tau may induce a peripheral inflammatory response in parallel with CNS immune alterations, suggesting that Abl activity and pathogenic proteins (p-Tau and α -Synuclein) function within a common loop; involving local communication between microglia and neurons and global crosstalk between body and CNS immunity. The current studies show age-dependent loss of immunosuppression via IL-10 and IL-4 and increase in caspase-3 activity in A53T brains. The early increase in IL-10 is perhaps due to an anti-inflammatory response, which is lost over time and results in decreased levels of the protective anti-inflammatory response at later stages of α -Synuclein accumulation. At least in the blood, IL-4 stimulates T-cell proliferation and induces differentiation of B cells into plasma cells, thus regulating humoral and adaptive immunity, while decreasing the production of TH1 macrophages, IFN- γ , and IL-12 [54–60]. The presence of IL-4 in extravascular tissues also promotes alternative activation of macrophages, which is coupled with secretion of IL-10 and diminution of inflammation [54–60]. In the brain, however, activation of microglia may either be beneficial or detrimental to neuronal survival. It is possible that the observed increase in activated amoeboid-like microglia in young A53T mice is an early event that leads to production of pro-inflammatory cytokines (IL-6 and IL-1 β) and caspase-3 activation [61], but modulation of the immune profile, via TKI, may result in ramified resting microglia phenotype [62], indicating a de-activated state. When microglia encounter α -

Synuclein or p-Tau they may actively change phenotype into a classical TH1 state, which is induced by TH1 cytokines such as IL-1, IL-6 and TNF α . A second state of activation associated with the TH2 cytokine profile of IL-4, IL-10, is the alternative activation state in which macrophages promote angiogenesis via increased VEGF levels. The ability of nilotinib and bosutinib to efficiently reduce p-Tau and α -Synuclein both centrally and peripherally may regulate microglia activation in A53T mice, leading to beneficial inflammatory response.

The decreased levels of IL-2 and IL-3 in A53T mice suggest loss of the immunological memory, leading to alterations of adaptive immunity. IL-3 is secreted by basophils and activated T cells to support growth and differentiation of multipotent hematopoietic stem cells into myeloid or lymphoid progenitor cells [37]. In addition, IL-3 stimulates proliferation of granulocytes, monocytes, and dendritic cells [37]. Activated T cells can either induce their own, and that of other, proliferation and differentiation of T cells in collaboration with IL-2 [63,64]. IL-2 is normally produced by T cells during an immune response [65,66]. For example, antigen binding to T cell receptors stimulates the secretion of IL-2 and survival of antigen-specific CD4⁺ and CD8⁺ T cells [67–69]. As such, IL-2 and IL-3 are necessary for the development of T cell immunologic memory, which depends upon the expansion of the number and function of antigen-selected T cell clones. Furthermore, IFN- γ activates macrophages and it is critical for innate and adaptive immunity against viral and intracellular bacterial infections and for tumor control; and its aberrant expression is associated with autoimmune diseases [38,39]. Therefore, the importance of IFN- γ in the immune system is its immunomodulatory effects, which seem to be suppressed in the brain and blood of A53T mice. Furthermore, IFN- γ is produced predominantly by natural killer cells as part of the innate immune response, and by CD4 Th1 and CD8 cytotoxic T cells once antigen-specific immunity develops [38,39]. However, despite the increased level of α -Synuclein and p-Tau in the blood and other tissues, including muscle and small intestine, no endogenous antibodies seem to be produced via T cell activation to protect against the pathogenic increase in amyloid protein in the blood or the brain. This suggests that T cells are either assured that the pathogenic species are not ‘foreign invaders’ or antigenic, or the immune system is incapable of mounting a protective strategy to degrade or eliminate α -Synuclein and p-Tau. However, the non-immunological autophagic clearance of amyloids with nilotinib and bosutinib may restrain the inflammatory response in the absence of immunological memory.

Chemokine brain levels, including CCL2 and CCL5 was decreased, but CX3CL1 concentration remained high independent of the effects of TKI, suggesting altered chemotactic activity in the brain and blood of A53T mice. CCL2 is involved in the neuroinflammatory processes that take place in neurodegeneration [70]. CCL5 recruits T cells, eosinophils, basophils, and leukocytes into inflammatory sites, and induces the proliferation and activation of certain natural-killer cells with the help of particular T-cell-released IL-2 and IFN- γ [47,48]. Therefore, the simultaneous decrease in CCL2, CCL5 as well as IL-2 and IFN- γ , suggests a vicious cycle that reflects failure of immunological counteraction of α -Synuclein and p-Tau in A53T mice. CCL2 and CCL5 play a crucial role in the brain, but their alterations have not been well studied in systemic immunity in neurodegenerative diseases. CCL2 is expressed by neurons throughout the brain [71] and its

expression level in glial cells is increased in epilepsy [72,73], brain ischemia [74], AD [75], experimental autoimmune encephalomyelitis (EAE) [76], and traumatic brain injury (TBI) [77]. CCL5 is a Human Immunodeficiency Virus (HIV)-suppressive factor released from CD8⁺ cells [78] and it is implicated in several human diseases [79–82].

It is important to note that the constantly elevated level of CX3CL1 was only decreased in the brain, but not in the blood, in A53T mice treated with nilotinib and bosutinib, suggesting that autophagic clearance of α -Synuclein and p-Tau may lead to attenuation of brain CX3CL1 level. The relationship between CX3CL1 and microglia activity has been extensively studied in several models of neurodegeneration, but fluctuations of soluble blood CX3CL1 have not been demonstrated in previous studies. We previously demonstrated that CX3CL1 levels are differentially altered in Tau gene transfer animal models that also over-express murine phosphorylated α -Synuclein [11,83]. Neurons secrete CX3CL1 [84], which exists in both membrane-bound and soluble forms [85].

The membrane-bound CX3CL1 can serve as an adhesion molecule for leukocytes expressing the fractalkine receptor (CX3CR1) [86] and soluble CX3CL1 can function as both a pro-inflammatory chemo-attractant that activates receptive inflammatory cells [49,87] and an anti-inflammatory [88], neuro-protective agent that reduces neuronal apoptosis [89]. Several findings suggest that deletion of CX3CR1 increases microglia activity in models of acute and chronic neuronal injury [90–93]. Exogenous CX3CL1 is neuro-protective in some models of neuro-inflammation [94,95], and disruption of CX3CL1 signaling causes neurotoxicity in models of systemic inflammation, PD, and amyotrophic lateral sclerosis [96] but protects against neuronal loss in a mouse model of focal cerebral ischemia [97]. Although the relationship between soluble CX3CL1 in peripheral blood and inflammatory diseases of the CNS has not been studied, serum CX3CL1 is increased in patients with multiple sclerosis [89,98], TBI [99] and HIV with CNS complications [100].

In conclusion, these studies demonstrate that nilotinib and bosutinib can reduce the levels of α -Synuclein and p-Tau in peripheral tissues and inside the CNS, and are therapeutic candidates to treat gastrointestinal complications in α -Synucleinopathies and other neurodegenerative diseases. Decreased inflammation may also contribute to less protein accumulation. TKIs may also be used to modulate the peripheral immune profile, which may affect CNS immunity, providing a double-edged strategy to facilitate protein degradation and orchestrate the systemic and CNS inflammatory response, thus mediating beneficial regulation of innate and adaptive immunity. The differential effects of nilotinib and bosutinib on the immune profile may be attributed to their potency to inhibit Abl and/or Src and other tyrosine kinases [34,35]. Finally, Abl and other TKIs should be explored as anti-inflammatory agents that provide combined effects, including amyloid clearance and anti-inflammation in neurodegenerative diseases.

Acknowledgments

These studies were supported by Georgetown University funding and NIH grants (NIA AG30378) to Charbel E-H Moussa.

References

1. Akiyama H, Barger S, Barnum S, Bradt B, Bauer J, et al. Inflammation and Alzheimer's disease. *Neurobiol Aging*. 2000; 21:383–421. [PubMed: 10858586]
2. Roodveldt C, Christodoulou J, Dobson CM. Immunological features of alpha-synuclein in Parkinson's disease. *J Cell Mol Med*. 2008; 12:1820–1829. [PubMed: 18671754]
3. Reynolds AD, Kadiu I, Garg SK, Glanzer JG, Nordgren T, et al. Nitrated alpha-synuclein and microglial neuroregulatory activities. *J Neuroimmune Pharmacol*. 2008; 3:59–74. [PubMed: 18202920]
4. Zhang W, Wang T, Pei Z, Miller DS, Wu X, et al. Aggregated alpha-synuclein activates microglia: a process leading to disease progression in Parkinson's disease. *FASEB J*. 2005; 19:533–542. [PubMed: 15791003]
5. Reynolds AD, Banerjee R, Liu J, Gendelman HE, Mosley RL. Neuroprotective activities of CD4+CD25+ regulatory T cells in an animal model of Parkinson's disease. *J Leukoc Biol*. 2007; 82:1083–1094. [PubMed: 17675560]
6. Su X, Maguire-Zeiss KA, Giuliano R, Prifti L, Venkatesh K, et al. Synuclein activates microglia in a model of Parkinson's disease. *Neurobiol Aging*. 2008; 29:1690–1701. [PubMed: 17537546]
7. Gebicke-Haerter PJ. Microglia in neurodegeneration: molecular aspects. *Microsc Res Tech*. 2001; 54:47–58. [PubMed: 11526957]
8. Gerhard A, Pavese N, Hotton G, Turkheimer F, Es M, et al. In vivo imaging of microglial activation with [¹¹C](R)-PK11195 PET in idiopathic Parkinson's disease. *Neurobiol Dis*. 2006; 21:404–412. [PubMed: 16182554]
9. Ishizawa K, Dickson DW. Microglial activation parallels system degeneration in progressive supranuclear palsy and corticobasal degeneration. *J Neuropathol Exp Neurol*. 2001; 60:647–657. [PubMed: 11398841]
10. Khandelwal PJ, Dumanis SB, Feng LR, Maguire-Zeiss K, Rebeck G, et al. Parkinson-related parkin reduces alpha-Synuclein phosphorylation in a gene transfer model. *Mol Neurodegener*. 2010; 5:47. [PubMed: 21050448]
11. Khandelwal PJ, Dumanis SB, Herman AM, Rebeck GW, Moussa CE. Wild type and P301L mutant Tau promote neuro-inflammation and alpha-Synuclein accumulation in lentiviral gene delivery models. *Mol Cell Neurosci*. 2012; 49:44–53. [PubMed: 21945393]
12. Li Y, Liu L, Barger SW, Griffin WS. Interleukin-1 mediates pathological effects of microglia on tau phosphorylation and on synaptophysin synthesis in cortical neurons through a p38-MAPK pathway. *J Neurosci*. 2003; 23:1605–1611. [PubMed: 12629164]
13. Quintanilla RA, Orellana DI, Gonzalez-Billault C, Maccioni RB. Interleukin-6 induces Alzheimer-type phosphorylation of tau protein by deregulating the cdk5/p35 pathway. *Exp Cell Res*. 2004; 295:245–257. [PubMed: 15051507]
14. Saez TE, Pehar M, Vargas M, Barbeito L, Maccioni RB. Astrocytic nitric oxide triggers tau hyperphosphorylation in hippocampal neurons. *In Vivo*. 2004; 18:275–280. [PubMed: 15341183]
15. Kitazawa M, Yamasaki TR, LaFerla FM. Microglia as a potential bridge between the amyloid beta-peptide and tau. *Ann N Y Acad Sci*. 2004; 1035:85–103. [PubMed: 15681802]
16. Yoshiyama Y, Higuchi M, Zhang B, Huang SM, Iwata N, et al. Synapse loss and microglial activation precede tangles in a P301S tauopathy mouse model. *Neuron*. 2007; 53:337–351. [PubMed: 17270732]
17. Schlatterer SD, Suh HS, Conejero-Goldberg C, Chen S, Acker CM, et al. Neuronal c-Abl activation leads to induction of cell cycle and interferon signaling pathways. *J Neuroinflammation*. 2012; 9:208. [PubMed: 22938163]
18. Schlatterer SD, Acker CM, Davies P. c-Abl in neurodegenerative disease. *J Mol Neurosci*. 2011; 45:445–452. [PubMed: 21728062]
19. Schlatterer SD, Tremblay MA, Acker CM, Davies P. Neuronal cAbl overexpression leads to neuronal loss and neuroinflammation in the mouse forebrain. *J Alzheimers Dis*. 2011; 25:119–133. [PubMed: 21368377]
20. Hebron ML, Lonskaya I, Moussa CE. Tyrosine kinase inhibition facilitates autophagic SNCA/alpha-synuclein clearance. *Autophagy*. 2013; 9:1249–1250. [PubMed: 23787811]

21. Hebron ML, Lonskaya I, Moussa CE. Nilotinib reverses loss of dopamine neurons and improves motor behavior via autophagic degradation of alpha-synuclein in Parkinson's disease models. *Hum Mol Genet.* 2013; 22:3315–3328. [PubMed: 23666528]
22. Mahul-Mellier AL, Fauvet B, Gysbers A, Dikiy I, Oueslati A, et al. c-Abl phosphorylates alpha-synuclein and regulates its degradation: implication for alpha-synuclein clearance and contribution to the pathogenesis of Parkinson's disease. *Hum Mol Genet.* 2014; 23:2858–2879. [PubMed: 24412932]
23. Schlatterer SD, Acker CM, Davies P. c-Abl in neurodegenerative disease. *J Mol Neurosci.* 2011; 45:445–452. [PubMed: 21728062]
24. Tremblay MA, Acker CM, Davies P. Tau phosphorylated at tyrosine 394 is found in Alzheimer's disease tangles and can be a product of the Abl-related kinase, Arg. *J Alzheimers Dis.* 2010; 19:721–733. [PubMed: 20110615]
25. Derkinderen P, Scales TM, Hanger DP, Leung KY, Byers HL, et al. Tyrosine 394 is phosphorylated in Alzheimer's paired helical filament tau and in fetal tau with c-Abl as the candidate tyrosine kinase. *J Neurosci.* 2005; 25:6584–6593. [PubMed: 16014719]
26. Jing Z, Caltagarone J, Bowser R. Altered subcellular distribution of c-Abl in Alzheimer's disease. *J Alzheimers Dis.* 2009; 17:409–422. [PubMed: 19363261]
27. Ittner LM, Ke YD, Delerue F, Bi M, Gladbach A, et al. Dendritic function of tau mediates amyloid-beta toxicity in Alzheimer's disease mouse models. *Cell.* 2010; 142:387–397. [PubMed: 20655099]
28. Reynolds CH, Garwood CJ, Wray S, Price C, Kellie S, et al. Phosphorylation regulates tau interactions with Src homology 3 domains of phosphatidylinositol 3-kinase, phospholipase Cgamma, Grb2, and Src family kinases. *J Biol Chem.* 2008; 283:18177–18186. [PubMed: 18467332]
29. Lee G. Tau and src family tyrosine kinases. *Biochim Biophys Acta.* 2005; 1739:323–330. [PubMed: 15615649]
30. Lonskaya I, Desforgues NM, Hebron ML, Moussa CE. Ubiquitination increases parkin activity to promote autophagic alpha-synuclein clearance. *PLoS One.* 2013; 8:e83914. [PubMed: 24386307]
31. Lonskaya I, Hebron ML, Algarzae NK, Desforgues N, Moussa CE. Decreased parkin solubility is associated with impairment of autophagy in the nigrostriatum of sporadic Parkinson's disease. *Neuroscience.* 2012; 232C:90. [PubMed: 23262240]
32. Lonskaya I, Hebron ML, Desforgues NM, Franjie A, Moussa CE. Tyrosine kinase inhibition increases functional parkin-Beclin-1 interaction and enhances amyloid clearance and cognitive performance. *EMBO Mol Med.* 2013; 5:1247–1262. [PubMed: 23737459]
33. Lonskaya I, Hebron ML, Desforgues NM, Schachter JB, Moussa CE. Nilotinib-induced autophagic changes increase endogenous parkin level and ubiquitination, leading to amyloid clearance. *J Mol Med (Berl).* 2014; 92:373–386. [PubMed: 24337465]
34. Kantarjian HM, Giles F, Gattermann N, Bhalla K, Alimena G, et al. Nilotinib (formerly AMN107), a highly selective BCR-ABL tyrosine kinase inhibitor, is effective in patients with Philadelphia chromosome-positive chronic myelogenous leukemia in chronic phase following imatinib resistance and intolerance. *Blood.* 2007; 110:3540–3546. [PubMed: 17715389]
35. Musumeci F, Schenone S, Brullo C, Botta M. An update on dual Src/Abl inhibitors. *Future Med Chem.* 2012; 4:799–822. [PubMed: 22530642]
36. Giasson BI, Duda JE, Quinn SM, Zhang B, Trojanowski JQ, et al. Neuronal alpha-synucleinopathy with severe movement disorder in mice expressing A53T human alpha-synuclein. *Neuron.* 2002; 34:521–533. [PubMed: 12062037]
37. Ihle JN, Pepersack L, Rebar L. Regulation of T cell differentiation: in vitro induction of 20 alpha-hydroxysteroid dehydrogenase in splenic lymphocytes from athymic mice by a unique lymphokine. *J Immunol.* 1981; 126:2184–2189. [PubMed: 6971890]
38. Naylor SL, Sakaguchi AY, Shows TB, Law ML, Goeddel DV, et al. Human immune interferon gene is located on chromosome 12. *J Exp Med.* 1983; 157:1020–1027. [PubMed: 6403645]
39. Schoenborn JR, Wilson CB. Regulation of interferon-gamma during innate and adaptive immune responses. *Adv Immunol.* 2007; 96:41–101. [PubMed: 17981204]

40. Shin YJ, Choi JS, Choi JY, Hou Y, Cha JH, et al. Induction of vascular endothelial growth factor receptor-3 mRNA in glial cells following focal cerebral ischemia in rats. *J Neuroimmunol.* 2010; 229:81–90. [PubMed: 20692049]
41. Rosenfeld PJ, Brown DM, Heier JS, Boyer DS, Kaiser PK, et al. Ranibizumab for neovascular age-related macular degeneration. *N Engl J Med.* 2006; 355:1419–1431. [PubMed: 17021318]
42. Machein MR, Plate KH. Role of VEGF in developmental angiogenesis and in tumor angiogenesis in the brain. *Cancer Treat Res.* 2004; 117:191–218. [PubMed: 15015562]
43. Storkebaum E, Lambrechts D, Carmeliet P. VEGF: once regarded as a specific angiogenic factor, now implicated in neuroprotection. *Bioessays.* 2004; 26:943–954. [PubMed: 15351965]
44. Lambrechts D, Carmeliet P. VEGF at the neurovascular interface: therapeutic implications for motor neuron disease. *Biochim Biophys Acta.* 2006; 1762:1109–1121. [PubMed: 16784838]
45. Carr MW, Roth SJ, Luther E, Rose SS, Springer TA. Monocyte chemoattractant protein 1 acts as a T-lymphocyte chemoattractant. *Proc Natl Acad Sci U S A.* 1994; 91:3652–3656. [PubMed: 8170963]
46. Xu LL, Warren MK, Rose WL, Gong W, Wang JM. Human recombinant monocyte chemotactic protein and other C-C chemokines bind and induce directional migration of dendritic cells in vitro. *J Leukoc Biol.* 1996; 60:365–371. [PubMed: 8830793]
47. Maghazachi AA, Al-Aoukaty A, Schall TJ. CC chemokines induce the generation of killer cells from CD56+ cells. *Eur J Immunol.* 1996; 26:315–319. [PubMed: 8617297]
48. Vangelista L, Secchi M, Liu X, Bachi A, Jia L, et al. Engineering of *Lactobacillus jensenii* to secrete RANTES and a CCR5 antagonist analogue as live HIV-1 blockers. *Antimicrob Agents Chemother.* 2010; 54:2994–3001. [PubMed: 20479208]
49. Pan Y, Lloyd C, Zhou H, Dolich S, Deeds J, et al. Neurotactin, a membrane-anchored chemokine upregulated in brain inflammation. *Nature.* 1997; 387:611–617. [PubMed: 9177350]
50. Pabon MM, Bachstetter AD, Hudson CE, Gemma C, Bickford PC. CX3CL1 reduces neurotoxicity and microglial activation in a rat model of Parkinson's disease. *J Neuroinflammation.* 2011; 8:9. [PubMed: 21266082]
51. Shan S, Hong-Min T, Yi F, Jun-Peng G, Yue F, et al. New evidences for fractalkine/CX3CL1 involved in substantia nigral microglial activation and behavioral changes in a rat model of Parkinson's disease. *Neurobiol Aging.* 2011; 32:443–458. [PubMed: 19368990]
52. Lee S, Varvel NH, Konerth ME, Xu G, Cardona AE, et al. CX3CR1 deficiency alters microglial activation and reduces beta-amyloid deposition in two Alzheimer's disease mouse models. *Am J Pathol.* 2010; 177:2549–2562. [PubMed: 20864679]
53. Fuhrmann M, Bittner T, Jung CK, Burgold S, Page RM, et al. Microglial Cx3cr1 knockout prevents neuron loss in a mouse model of Alzheimer's disease. *Nat Neurosci.* 2010; 13:411–413. [PubMed: 20305648]
54. Apte SH, Baz A, Groves P, Kelso A, Kienzle N. Interferon-gamma and interleukin-4 reciprocally regulate CD8 expression in CD8+ T cells. *Proc Natl Acad Sci U S A.* 2008; 105:17475–17480. [PubMed: 18988742]
55. Sokol CL, Barton GM, Farr AG, Medzhitov R. A mechanism for the initiation of allergen-induced T helper type 2 responses. *Nat Immunol.* 2008; 9:310–318. [PubMed: 18300366]
56. Maes T, Joos GF, Brusselle GG. Targeting interleukin-4 in asthma: lost in translation? *Am J Respir Cell Mol Biol.* 2012; 47:261–270. [PubMed: 22538865]
57. Chatila TA. Interleukin-4 receptor signaling pathways in asthma pathogenesis. *Trends Mol Med.* 2004; 10:493–499. [PubMed: 15464449]
58. Howard M, Paul WE. Interleukins for B lymphocytes. *Lymphokine Res.* 1982; 1:1–4. [PubMed: 6985399]
59. Yokota T, Otsuka T, Mosmann T, Banchereau J, DeFrance T, et al. Isolation and characterization of a human interleukin cDNA clone, homologous to mouse B-cell stimulatory factor, that expresses B-cell- and T-cell-stimulating activities. *Proc Natl Acad Sci U S A.* 1986; 83:5894–5898. [PubMed: 3016727]
60. Marone G, Florio G, Petraroli A, de Paulis A. Dysregulation of the IgE/Fc epsilon RI network in HIV-1 infection. *J Allergy Clin Immunol.* 2001; 107:22–30. [PubMed: 11149986]

61. Filipov NM, Seegal RF, Lawrence DA. Manganese potentiates in vitro production of proinflammatory cytokines and nitric oxide by microglia through a nuclear factor kappa B-dependent mechanism. *Toxicol Sci.* 2005; 84:139–148. [PubMed: 15601679]
62. Lumeng CN, Bodzin JL, Saltiel AR. Obesity induces a phenotypic switch in adipose tissue macrophage polarization. *J Clin Invest.* 2007; 117:175–184. [PubMed: 17200717]
63. Yang YC, Ciarletta AB, Temple PA, Chung MP, Kovacic S, et al. Human IL-3 (multi-CSF): identification by expression cloning of a novel hematopoietic growth factor related to murine IL-3. *Cell.* 1986; 47:3–10. [PubMed: 3489530]
64. Obituaries: Mrs Annie Isabella Anslow, Eileen Georgina Sherrard. *N Z Nurs J.* 1979; 72:32–33. No authors listed. [PubMed: 395466]
65. Cantrell DA, Smith KA. The interleukin-2 T-cell system: a new cell growth model. *Science.* 1984; 224:1312–1316. [PubMed: 6427923]
66. Smith KA. Interleukin-2: inception, impact, and implications. *Science.* 1988; 240:1169–1176. [PubMed: 3131876]
67. Stern JB, Smith KA. Interleukin-2 induction of T-cell G1 progression and c-myc expression. *Science.* 1986; 233:203–206. [PubMed: 3523754]
68. Beadling C, Johnson KW, Smith KA. Isolation of interleukin 2-induced immediate-early genes. *Proc Natl Acad Sci U S A.* 1993; 90:2719–2723. [PubMed: 7681987]
69. Beadling C, Smith KA. DNA array analysis of interleukin-2-regulated immediate/early genes. *Med Immunol.* 2002; 1:2. [PubMed: 12459040]
70. Gerard C, Rollins BJ. Chemokines and disease. *Nat Immunol.* 2001; 2:108–115. [PubMed: 11175802]
71. Banisadr G, Gosselin RD, Mechighel P, Kitabgi P, Rostene W, et al. Highly regionalized neuronal expression of monocyte chemoattractant protein-1 (MCP-1/CCL2) in rat brain: evidence for its colocalization with neurotransmitters and neuropeptides. *J Comp Neurol.* 2005; 489:275–292. [PubMed: 16025454]
72. Foresti ML, Arisi GM, Katki K, Montanez A, Sanchez RM, et al. Chemokine CCL2 and its receptor CCR2 are increased in the hippocampus following pilocarpine-induced status epilepticus. *J Neuroinflammation.* 2009; 6:40. [PubMed: 20034406]
73. Fabene PF, Bramanti P, Constantin G. The emerging role for chemokines in epilepsy. *J Neuroimmunol.* 2010; 224:22–27. [PubMed: 20542576]
74. Kim JS, Gautam SC, Chopp M, Zaloga C, Jones ML, et al. Expression of monocyte chemoattractant protein-1 and macrophage inflammatory protein-1 after focal cerebral ischemia in the rat. *J Neuroimmunol.* 1995; 56:127–134. [PubMed: 7860708]
75. Hickman SE, El Khoury J. Mechanisms of mononuclear phagocyte recruitment in Alzheimer's disease. *CNS Neurol Disord Drug Targets.* 2010; 9:168–173. [PubMed: 20205643]
76. Ransohoff RM, Hamilton TA, Tani M, Stoler MH, Shick HE, et al. Astrocyte expression of mRNA encoding cytokines IP-10 and JE/MCP-1 in experimental autoimmune encephalomyelitis. *FASEB J.* 1993; 7:592–600. [PubMed: 8472896]
77. Semple BD, Bye N, Rancan M, Ziebell JM, Morganti-Kossmann MC. Role of CCL2 (MCP-1) in traumatic brain injury (TBI): evidence from severe TBI patients and CCL2^{-/-} mice. *J Cereb Blood Flow Metab.* 2010; 30:769–782. [PubMed: 20029451]
78. Cocchi F, DeVico AL, Garzino-Demo A, Arya SK, Gallo RC, et al. Identification of RANTES, MIP-1 alpha, and MIP-1 beta as the major HIV-suppressive factors produced by CD8⁺ T cells. *Science.* 1995; 270:1811–1815. [PubMed: 8525373]
79. Struyf S, Menten P, Lenaerts JP, Put W, D'Haese A, et al. Diverging binding capacities of natural LD78beta isoforms of macrophage inflammatory protein-1alpha to the CC chemokine receptors, 3 and 5 affect their anti-HIV-1 activity and chemotactic potencies for neutrophils and eosinophils. *Eur J Immunol.* 2001; 31:2170–2178. [PubMed: 11449371]
80. Schall TJ, Jongstra J, Dyer BJ, Jorgensen J, Clayberger C, et al. A human T cell-specific molecule is a member of a new gene family. *J Immunol.* 1988; 141:1018–1025. [PubMed: 2456327]
81. Song A, Chen YF, Thamtrakoln K, Storm TA, Krensky AM. RFLAT-1: a new zinc finger transcription factor that activates RANTES gene expression in T lymphocytes. *Immunity.* 1999; 10:93–103. [PubMed: 10023774]

82. Song A, Nikolcheva T, Krensky AM. Transcriptional regulation of RANTES expression in T lymphocytes. *Immunol Rev.* 2000; 177:236–245. [PubMed: 11138780]
83. Hebron ML, Algarzae NK, Lonskaya I2, Moussa C3. Fractalkine signaling and Tau hyperphosphorylation are associated with autophagic alterations in lentiviral Tau and AI21–42 gene transfer models. *Exp Neurol.* 2014; 251:127–138. [PubMed: 23333589]
84. Harrison JK, Jiang Y, Chen S, Xia Y, Maciejewski D, et al. Role for neuronally derived fractalkine in mediating interactions between neurons and CX3CR1-expressing microglia. *Proc Natl Acad Sci U S A.* 1998; 95:10896–10901. [PubMed: 9724801]
85. Hatori K, Nagai A, Heisel R, Ryu JK, Kim SU. Fractalkine and fractalkine receptors in human neurons and glial cells. *J Neurosci Res.* 2002; 69:418–426. [PubMed: 12125082]
86. Imai T, Hieshima K, Haskell C, Baba M, Nagira M, et al. Identification and molecular characterization of fractalkine receptor CX3CR, which mediates both leukocyte migration and adhesion. *Cell.* 1997; 91:521–530. [PubMed: 9390561]
87. Bazan JF, Bacon KB, Hardiman G, Wang W, Soo K, et al. A new class of membrane-bound chemokine with a CX3C motif. *Nature.* 1997; 385:640–644. [PubMed: 9024663]
88. Yoneda O, Imai T, Goda S, Inoue H, Yamauchi A, et al. Fractalkine-mediated endothelial cell injury by NK cells. *J Immunol.* 2000; 164:4055–4062. [PubMed: 10754298]
89. Tong N, Perry SW, Zhang Q, James HJ, Guo H, et al. Neuronal fractalkine expression in HIV-1 encephalitis: roles for macrophage recruitment and neuroprotection in the central nervous system. *J Immunol.* 2000; 164:1333–1339. [PubMed: 10640747]
90. Bhaskar K, Konerth M, Kokiko-Cochran ON, Cardona A, Ransohoff RM, et al. Regulation of tau pathology by the microglial fractalkine receptor. *Neuron.* 2010; 68:19–31. [PubMed: 20920788]
91. Cardona AE, Sasse ME, Liu L, Cardona SM, Mizutani M, et al. Scavenging roles of chemokine receptors: chemokine receptor deficiency is associated with increased levels of ligand in circulation and tissues. *Blood.* 2008; 112:256–263. [PubMed: 18347198]
92. Liu Z, Condello C, Schain A, Harb R, Grutzendler J. CX3CR1 in microglia regulates brain amyloid deposition through selective protofibrillar amyloid-I2 phagocytosis. *J Neurosci.* 2010; 30:17091–17101. [PubMed: 21159979]
93. Cho SH, Sun B, Zhou Y, Kauppinen TM, Halabisky B, et al. CX3CR1 protein signaling modulates microglial activation and protects against plaque-independent cognitive deficits in a mouse model of Alzheimer disease. *J Biol Chem.* 2011; 286:32713–32722. [PubMed: 21771791]
94. Meucci O, Fatatis A, Simen AA, Bushell TJ, Gray PW, et al. Chemokines regulate hippocampal neuronal signaling and gp120 neurotoxicity. *Proc Natl Acad Sci U S A.* 1998; 95:14500–14505. [PubMed: 9826729]
95. Mizuno T, Kawanokuchi J, Numata K, Suzumura A. Production and neuroprotective functions of fractalkine in the central nervous system. *Brain Res.* 2003; 979:65–70. [PubMed: 12850572]
96. Cardona AE, Pioro EP, Sasse ME, Kostenko V, Cardona SM, et al. Control of microglial neurotoxicity by the fractalkine receptor. *Nat Neurosci.* 2006; 9:917–924. [PubMed: 16732273]
97. Denes A, Ferenczi S, Halasz J, Kornyei Z, Kovacs KJ. Role of CX3CR1 (fractalkine receptor) in brain damage and inflammation induced by focal cerebral ischemia in mouse. *J Cereb Blood Flow Metab.* 2008; 28:1707–1721. [PubMed: 18575457]
98. Kastenbauer S, Koedel U, Wick M, Kieseier BC, Hartung HP, et al. CSF and serum levels of soluble fractalkine (CX3CL1) in inflammatory diseases of the nervous system. *J Neuroimmunol.* 2003; 137:210–217. [PubMed: 12667665]
99. Rancan M, Bye N, Otto VI, Trentz O, Kossmann T, et al. The chemokine fractalkine in patients with severe traumatic brain injury and a mouse model of closed head injury. *J Cereb Blood Flow Metab.* 2004; 24:1110–1118. [PubMed: 15529011]
100. Sporer B, Kastenbauer S, Koedel U, Arendt G, Pfister HW. Increased intrathecal release of soluble fractalkine in HIV-infected patients. *AIDS Res Hum Retroviruses.* 2003; 19:111–116. [PubMed: 12639246]

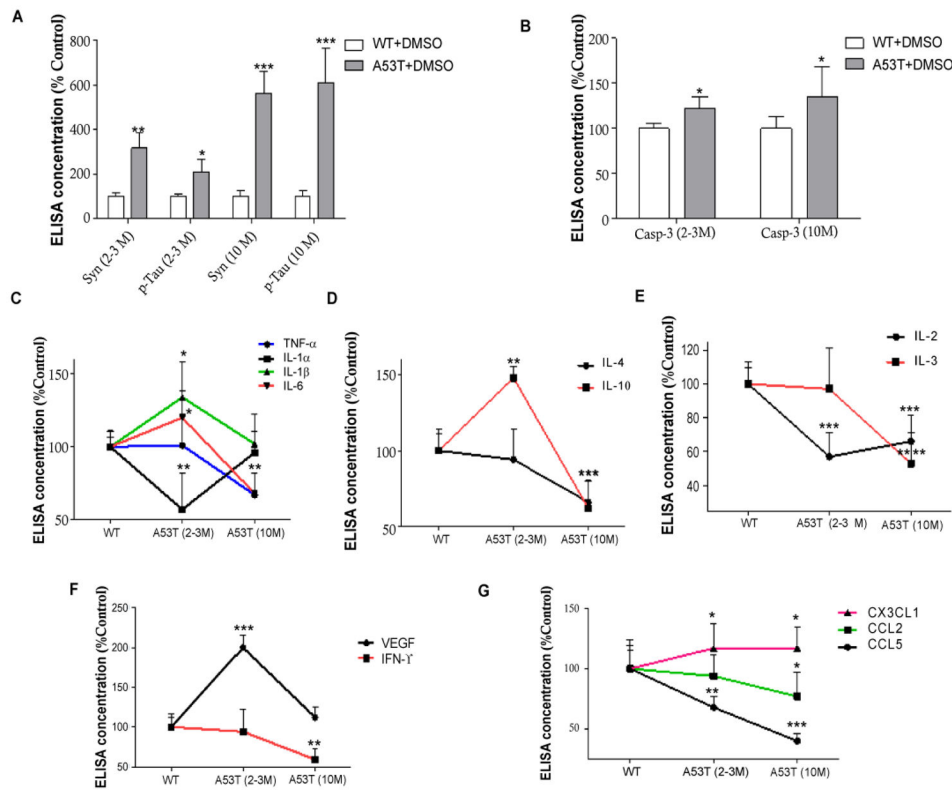
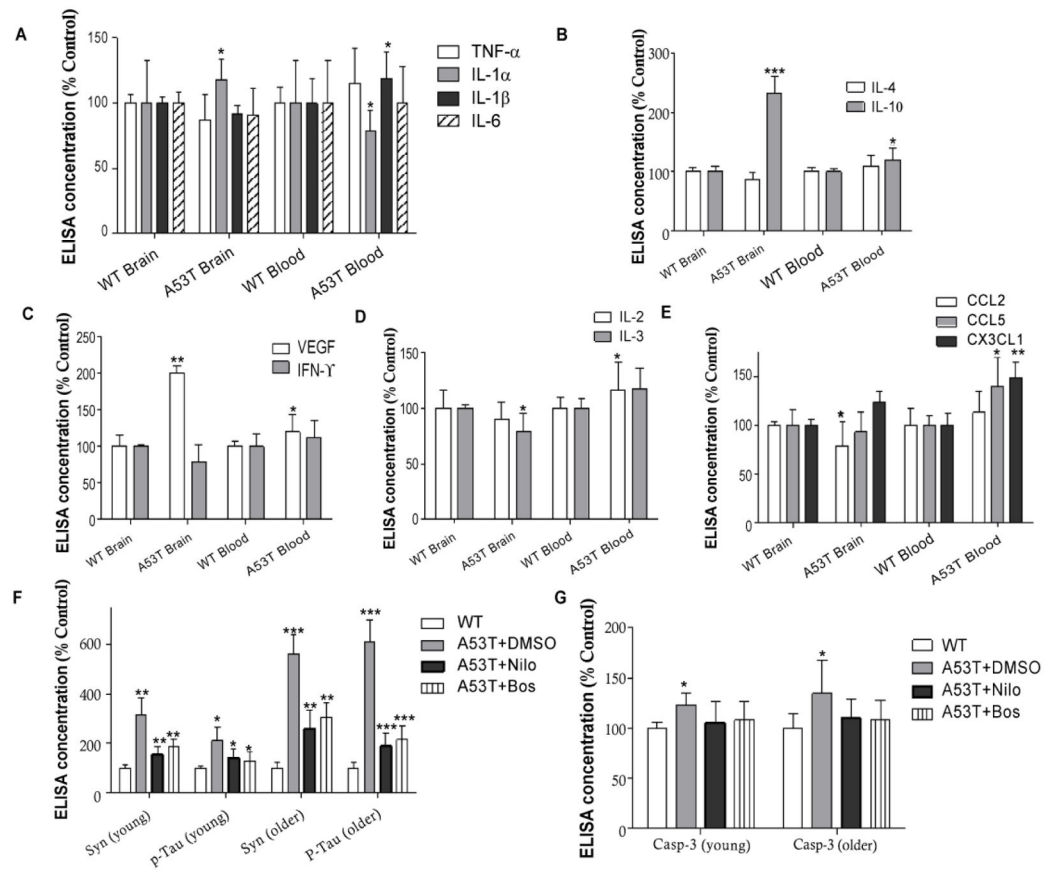


Figure 1. Age-dependent alterations of brain immunity in A53T mice

Histograms represent ELISA levels of **A)** α -Synuclein and p-Tau in the brain of A53T mice, and **B)** shows caspase-3 activity in young and older mice. Graphs represent the levels of mouse A53T brain immune markers, including **C)** pro-inflammatory IL-1 α , IL-1 β , IL-6 and TNF- α , **D)** anti-inflammatory IL-4 and IL-10, **E)** modulators of immune memory IL-2 and IL-3, **F)** VEGF and IFN- γ and **G)** chemokines CCL2, CCL5 and CX3CL1. $n=5$ for each strain at each time point. ANOVA, Neuman Keuls, Mean \pm SD, * indicates significantly different than WT with $p<0.05$, ** $p<0.01$, *** $p<0.001$, **** $p<0.0001$.



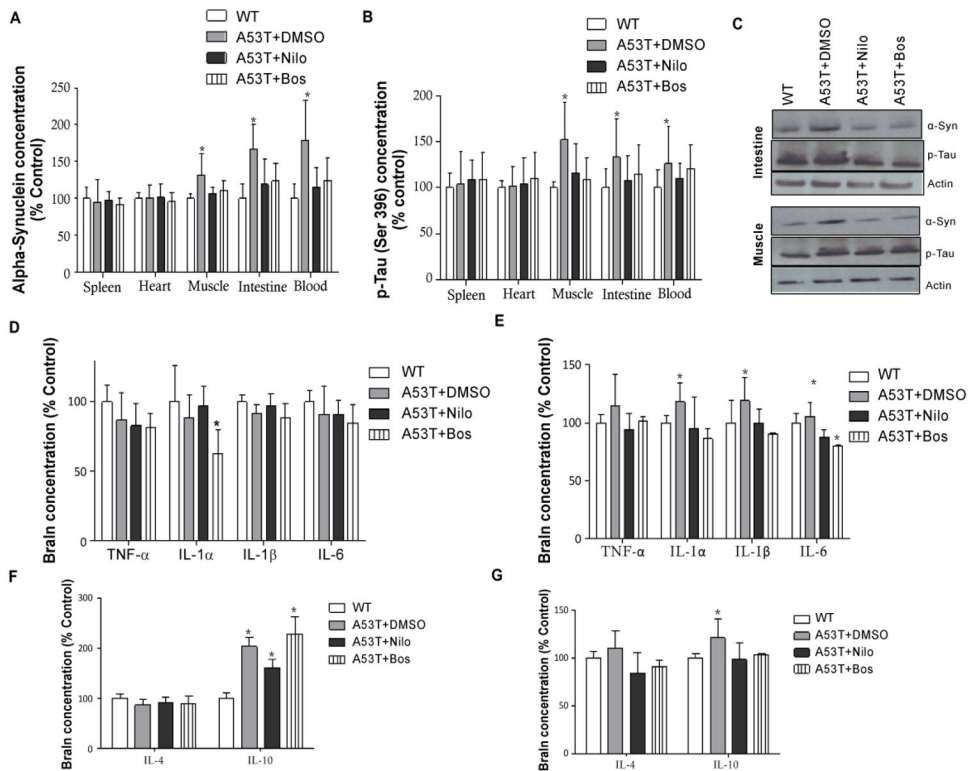


Figure 3. Nilotinib and bosutinib decrease CNS and peripheral levels of α -Synuclein and p-Tau and modulate cytokine levels

Histograms represent ELISA levels of **A)** α -Synuclein and **B)** p-Tau in the spleen, heart, muscle, intestine and blood of A53T mice treated I.P with 10 mg/kg nilotinib or 5 mg/kg bosutinib or 3 μ L DMSO every other day for 6 weeks. **C)** Western blot analysis on 10% S NuPAGE gel showing analysis of muscle and intestine homogenized in 1xSTEN buffer to compare nilotinib and bosutinib effects with DMSO in A53T mice. **D)** brain and **E)** blood levels of pro-inflammatory IL-1 α , IL-1 β , IL-6 and TNF- α . **F)** brain and **G)** blood levels of anti-inflammatory IL-4 and IL-10. n= 5 for each strain at each time point. ANOVA, Neuman Keuls, Mean \pm SD, * indicates significantly different than W, p<0.05.

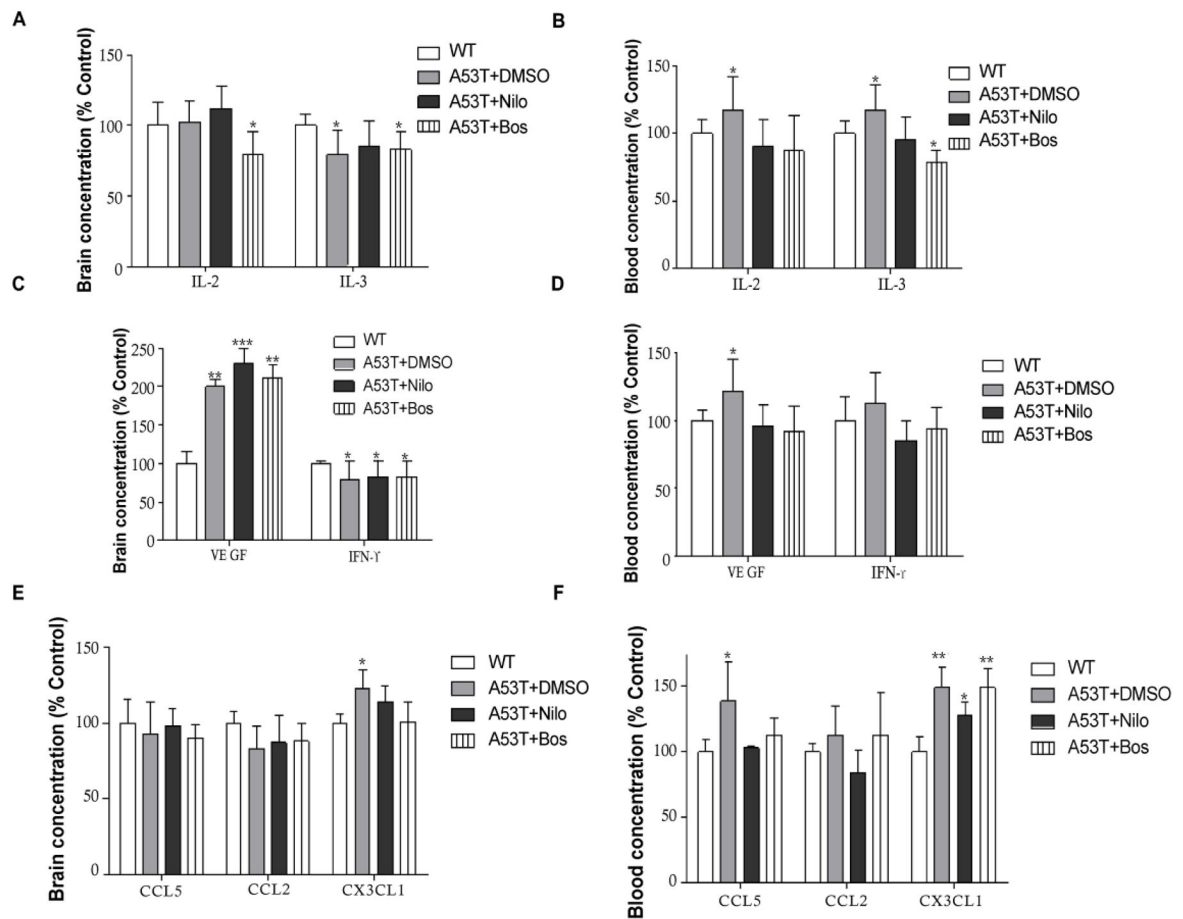


Figure 4. Nilotinib and bosutinib modulate changes in the blood immunological profiles of A53T mice

Histograms represent ELISA levels in A53T mice treated I.P with 10 mg/kg nilotinib or 5 mg/kg bosutinib or 3 μ L DMSO every other day for 6 weeks in **A**) brain and **B**) blood levels of modulators of immune memory IL-2 and IL3, **C**) brain and **D**) blood VEGF and IFN- γ and **E**) and **F**) blood levels chemokines CCL2, CCL5 and CX3CL1. n=5 for each strain at each time point. ANOVA, Neuman Keuls, Mean \pm SD, * indicates significantly different than WT with p<0.05, **p<0.01.

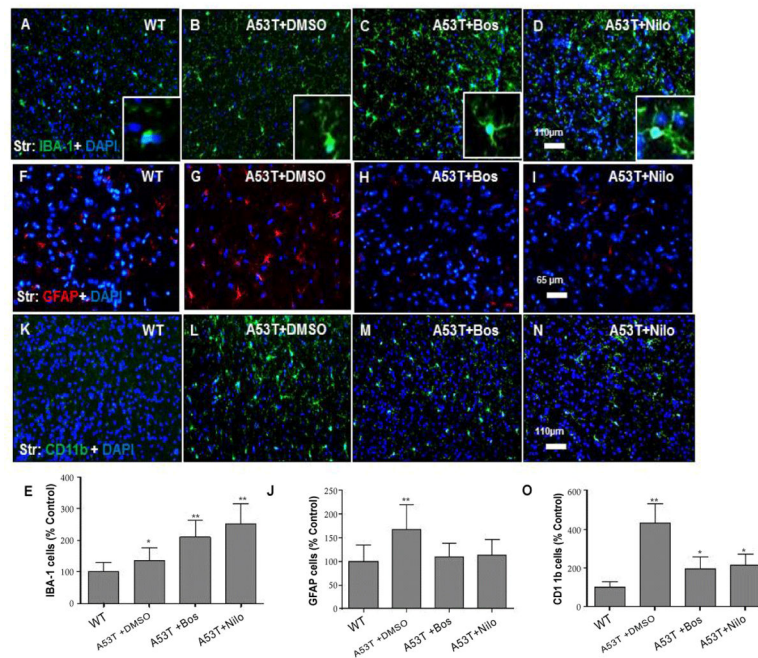


Figure 5. Nilotinib and bosutinib alter microglia morphology and reduce the number of astrocyte and dendritic cells

Coronal 20 μm thick brain sections show IBA-1 and nuclear DAPI staining of microglia in the striatum of **A)** WT mice, **B)** A53T mice treated with DMSO, insert is higher magnification, **C)** A53T mice treated with bosutinib, insert is higher magnification, and **D)** A53T mice treated with nilotinib, insert is higher magnification. **E)** histograms represent stereological quantification. Coronal 20 μm thick brain sections show GFAP and nuclear DAPI staining of astrocytes in the striatum of **F)** WT mice, **G)** A53T mice treated with DMSO, **H)** A53T mice treated with bosutinib, and **I)** A53T mice treated with nilotinib. **J)** histograms represent stereological quantification. Dendritic cells stained with CD11b and nuclear DAPI labeling in the striatum of **K)** WT mice, **L)** A53T mice treated with DMSO, **M)** A53T mice treated with bosutinib, and **N)** A53T mice treated with nilotinib. **O)** histograms represent stereological quantification. $n=5$ for each strain at each time point. $n=4$, ANOVA, Neuman Keuls, Mean \pm SD, * indicates significantly different than WT with $p<0.05$, ** $p<0.01$.